Optothermal Properties of Fiber Morphology on Nylon 66 Fibers Due to Annealing and Drawing Processes

I. M. FOUDA

Physics Department, Mansoura University, Mansoura, Egypt

Received 12 February 2001; accepted 29 May 2001

ABSTRACT: The changes produced by the effects of annealed and drawn fibers on the microstructure and macrostructure of nylon 66 fibers are considered. The optical properties and strain produced in nylon 66 fibers under different conditions are measured interferometrically at room temperature. Structural parameters are calculated such as the average work per chain, the work per unit volume, the reduction in entropy due to elongation, and the work stored in the body as strain energy. The evaluation of the density aided the calculation of the crystallinity, the mean square density fluctuation, the isotropic refractive index, the harmonic mean polarizability of the dielectric, and the harmonic mean specific refractivity. In addition, the resulting data are utilized to calculate the optical stress coefficient and the optical configuration and to apply the Mooney–Rivlin equation to determine its constants. Also, the number of crystals per unit volume and the average orientation angle for uniaxial stretching are calculated by the extension ratio. The relations between the optical, mechanical, and thermal changes with different parameters are given for the studied fibers. © 2002 Wiley Periodicals, Inc. J Appl Polym Sci 84: 916–928, 2002; DOI 10.1002/app.10107

Key words: optothermal properties; fiber morphology; nylon 66; annealing; drawing

INTRODUCTION

Optical, mechanical, thermal, and chemical treatments play important roles in the characterization of synthetic and natural fibers. Recently, application of two- or multiple-beam interference to determine the optical parameters led to accurate information on the correlation of the structural orientation to the properties of these fibers. The birefringence, orientation, density, crystallinity, entropy, and elasticity are some of the properties that affect textile quality for the main end use.[1–10]

Thus, thermal and mechanical treatments are used to vary the degree of orientation, crystallinity, and many other physical properties in polymeric materials. Also, to explain the different variations obtained due to thermomechanical effects, several structural processes interfered and should be taken into consideration, which are discussed elsewhere.[11–13]

Most studies, which involve the variation of the physical properties, considered polymers as an anisotropic polycrystalline medium, which consists of crystalline regions suspended in an amorphous medium that is partially oriented.

In this work the optical and calculated crystallinities for nylon 66 with different draw ratios (previously measured interferometrically using a two-beam Pluta interference microscope in conjunction with a microstrain device[14]) are utilized to calculate structural parameters. The relationships are given for the optical, mechanical, and structural parameters.

Correspondence to: I. M. Fouda (fsharkawy_2000@yahoo.com).

Journal of Applied Polymer Science, Vol. 84, 916–928 (2002)

THEORETICAL

The mean values of the refractive indices of the fiber and the total mean birefringence were calculated using the equations that were extensively used in our previous publications.[15–18] The Kuhen–Treloar type theory gives[19]

$$F_\theta = \frac{2}{5} N_c [D^2 - D^{-1}] \quad (1)$$

where F_θ is the Herman orientation function[20]; N_c is the number of chains per unit volume that depends on the number of crystallites in the polymer material; and D is the draw ratio, where $D = l_d/l_u$ and $D = 1 + d$, d is the strain, l_d is the fiber length before drawing, and l_u is the length after drawing.

$$F_\Delta = \frac{\Delta n}{\Delta n_{\max}} \quad (2)$$

where F_Δ is the ΔF and n and $n_{\max}$ are the changes in the refractive index and maximum n, respectively.

For an ideal network[22]

$$v = \frac{N_A \rho}{M} \quad (3)$$

where v is the number of network chains per unit volume, N_A is Avogadro's number, ρ is the polymer density for nylon 66, and M is the monomer molecular units (226 for the nylon 66 fibers).

Because the stress is related to the elongation by

$$\sigma = vkT[D - D^{-2}] \quad (4)$$

where σ is the stress, k is Boltzmann's constant, and T is the absolute temperature.

Also, the elongation leads to a reduction in the entropy (ΔS) by the following equation:

$$\Delta S = -\frac{1}{2} kv \left[(1 + d)^2 + \frac{2}{(1 + d)} - 3 \right] \quad (5)$$

The average work per chain (W') for a collection of chains will depend on the distribution of chain-end distances and is obtained by the following equation[23]:

$$W' = \frac{3kT}{2} \left| \frac{1}{3} (D^2 - D^{-1}) + (D^{-1} - 1) \right| \quad (6)$$

For a collection of chains containing v chains per unit volume, the work per unit volume (W) is given by

$$W = \frac{vkT}{2} [(D^2 - D^{-1}) + 3(D^{-1} - 1)] \quad (7)$$

The greatest difficulties in applying eqs. (5), (6), and (8) arise in assigning a suitable value to v and establishing the conditions to achieve equilibrium relaxation. In the present work these difficulties are not discussed. We also evaluate the densities for different draw ratios from eq. (3).

Mooney–Rivlin Equation

The storable, elastic energy of the network (W'') is only a function of the strain invariant. It can be represented by the following equation for a uniaxial elongation:

$$W'' = C_1[D^2 + 2D^{-1} - 3] + C_2[D^{-2} + 2D^{-3}] \quad (8)$$

and

$$\sigma = \frac{W''}{\partial D} = C_1[2D - 2D^{-2}] + C_2[2 - 2D^{-3}] \quad (9)$$

or

$$\sigma = 2[C_1 + C_2 D^{-1}][D - D^{-2}] \quad (10)$$

Equation (9) is the well known Mooney–Rivlin equation. A plot of the reduced stress $\sigma/2(D - D^{-2})$ as a function of the reciprocal elongation D^{-1} gives a straight line whose slope is C_2 and whose intercept with the ordinate is C_1. In practice the constant C_1 has proved to be a useful measure of the crosslink density. The second term is attributed to energy dissipation resulting from chain interactions during deformation, and in conformity with this view C_2 becomes zero when the elastomer is swollen by solvents.

Optical Stress Coefficient

The constant C_s is called the optical stress coefficient. The value of this coefficient is dependent on the chemical structure of the polymer. The value

of this coefficient also depends solely on the mean refractive index ($\bar{n}$) and the optical anisotropy of the random link as seen from the following equation:

$$C_s = \frac{2\pi}{45kT}\left[\frac{(\bar{n}^2+2)^2}{\bar{n}}\right][\alpha_\parallel - \alpha_\perp] \qquad (11)$$

where $\alpha^\parallel$ and $\alpha^\perp$ are the polarizabilities along and across the axis of such units, respectively; and C_s is independent of the chain length and the degree of crosslinking. From the above equation it can be seen that the birefringence in elastomers is proportional to the applied stress.

Calculation of Optical Configuration Parameter

The optical configuration parameter (Δa) is related to the C_s by the following equation[24]:

$$\Delta a = \frac{(45kTC_s/2\pi)\bar{n}}{(\bar{n}+2)^2} \qquad (12)$$

The values of Δa at different values of $\bar{n}$, C_s, and W'' are summarized in Tables I–III.

Calculation of Crystalline and Amorphous Orientation Functions

The amorphous orientation function (F_a) was calculated by combining the two models of Samuel and Gaylord for the crystalline orientation (F_c). The Gaylord model is in good agreement with the experimental data on nylon 66, as follows[25]:

$$\Delta n = \chi \Delta n_c F_c + (1-\chi)\Delta n_a F_a \qquad (13)$$

where χ is the degree of crystallinity, Δn_c is the crystalline n (0.074), Δn_a is the noncrystalline n (0.086), $F_c = (D^3 - 1)/(D^3 + 2)$, and D is for the line material.

The χ was determined by the relation

$$\chi = \frac{\rho - \rho_a}{\rho_c - \rho_a} \qquad (14)$$

where ρ_c and ρ_a are the densities of the crystalline (1.236 g/mL)[26] and noncrystalline (1.12 g/mL)[22] regions, respectively.

Table I

Draw Ratio	N_C	$N' \times 10^{23}$	$B \times 10^7$	$E \times 10^7$	$\sigma \times 10^7$	$C_s \times 10^{-7}$	$\Delta a \times 10^{-23}$	W''	R	$\delta^2 \times 10^3$	$\gamma_s \times 10^{-32}$	$\beta \times 10^{-7}$
1.000	—	—	—	—	—	—	—	—	—	—	—	—
1.167	3.70	2.37	0.804	0.345	0.049	1.112	2.641	0.159	0.069	0.316	2.93	1.24
1.333	1.92	1.84	0.409	0.306	0.078	0.744	1.768	0.111	0.078	0.225	1.96	2.44
1.500	1.38	1.57	0.294	0.294	0.103	0.624	1.488	0.093	0.081	0.191	1.65	3.40
1.667	1.11	1.37	0.238	0.286	0.124	0.576	1.377	0.106	0.082	0.172	1.53	4.19
1.833	0.85	1.23	0.207	0.282	0.144	0.491	1.172	0.128	0.084	0.160	1.30	4.83
1.917	0.79	1.23	0.204	0.294	0.161	0.458	1.097	0.142	0.080	0.159	1.22	4.88
2.000	0.79	1.49	0.248	0.372	0.217	0.377	0.905	0.157	0.063	0.175	1.00	4.02
2.083	0.76	1.37	0.229	0.357	0.221	0.392	0.941	0.174	0.065	0.168	1.04	4.36
2.170	0.70	1.27	0.212	0.343	0.224	0.393	0.944	0.194	0.068	0.162	1.05	4.71

Table II

Draw Ratio	N_C	$N' \times 10^{23}$	$B \times 10^{7}$	$E \times 10^{7}$	$\sigma \times 10^{7}$	$C_s \times 10^{-7}$	$\Delta a \times 10^{-7}$	W''	R	$\delta^2 \times 10^{3}$	$\gamma_s \times 10^{-32}$	$\beta \times 10^{-7}$
1.00	—	—	—	—	—	—	—	—	—	—	—	—
1.08	8.32	2.68	1.627	0.361	0.027	2.20	0.0525	0.150	0.065	0.449	5.84	0.61
1.16	4.45	2.42	0.845	0.349	0.048	1.305	0.0312	0.136	0.067	0.324	3.47	1.18
1.32	2.22	2.01	0.455	0.331	0.082	0.784	0.0187	0.109	0.072	0.238	2.08	2.19
1.48	1.45	1.73	0.328	0.319	0.109	0.596	0.0142	0.103	0.074	0.202	1.58	3.04
1.56	1.28	1.69	0.305	0.329	0.126	0.537	0.0128	0.105	0.071	0.195	1.43	3.27
1.96	0.71	1.16	0.194	0.285	0.161	0.432	0.0103	0.149	0.083	0.155	1.15	5.15
2.12	0.63	1.09	0.182	0.288	0.182	0.412	0.0098	0.179	0.082	0.150	1.09	5.50
2.28	0.55	0.94	0.159	0.268	0.186	0.414	0.0099	0.214	0.088	0.140	1.10	6.28
2.44	0.48	0.82	0.141	0.250	0.189	0.421	0.0100	0.253	0.094	0.132	1.11	7.07

Table III

Draw Ratio	N_C	$N' \times 10^{23}$	$B \times 10^{7}$	$E \times 10^{7}$	$\sigma \times 10^{7}$	$C_s \times 10^{-7}$	$\Delta a \times 10^{-23}$	W''	R	$\delta^2 \times 10^{3}$	$\gamma_s \times 10^{-32}$	$\beta \times 10^{-7}$
1.000	—	—	—	—	—	—	—	—	—	—	—	—
1.160	4.54	2.54	0.887	0.367	0.051	1.272	3.037	0.169	0.064	0.332	3.37	1.12
1.320	2.30	2.12	0.480	0.349	0.086	0.770	1.841	0.131	0.068	0.244	2.05	2.08
1.480	1.64	1.76	0.333	0.324	0.110	0.662	1.582	0.116	0.073	0.203	1.76	2.99
1.640	1.22	1.49	0.260	0.305	0.129	0.583	1.393	0.115	0.077	0.180	1.55	3.84
1.880	0.86	1.23	0.206	0.289	0.154	0.498	1.192	0.132	0.081	0.160	1.32	4.85
1.960	0.80	1.24	0.206	0.303	0.172	0.457	1.095	0.141	0.078	0.160	1.22	4.84
2.040	0.72	1.38	0.230	0.353	0.211	0.371	0.888	0.152	0.067	0.169	0.99	4.33
2.120	0.74	1.28	0.214	0.339	0.214	0.414	0.988	0.164	0.070	0.163	1.09	4.66

Table IV

Draw Ratio	$n_{iso(1)}$	$n_{iso(2)}$	F_a	ρ	χ (%)	$\langle\eta^2\rangle \times 10^{-2}$	tan θ'
1.000	1.555	1.553	0.6839	1.1226	2.288	3.01	0.6580
1.167	1.553	1.551	0.7612	1.1225	2.210	2.91	0.5219
1.333	1.552	1.550	0.8013	1.1225	2.165	2.85	0.4275
1.500	1.548	1.546	0.8805	1.1224	2.071	2.73	0.3581
1.667	1.543	1.542	0.9769	1.1222	1.945	2.57	0.3057
1.833	1.545	1.543	0.9625	1.1222	1.962	2.59	0.2651
1.917	1.543	1.541	1.0029	1.1222	1.906	2.52	0.2479
2.000	1.538	1.537	1.1133	1.1220	1.742	2.30	0.2326
2.083	1.538	1.537	1.1757	1.1219	1.645	2.18	0.2188
2.170	1.539	1.537	1.1970	1.1218	1.611	2.13	0.2058

Mean Square Density Fluctuation

For undrawn and drawn nylon 66 fibers, the mean square density fluctuation ($\langle\eta^2\rangle$) can be calculated from the following equation[27]:

$$\langle\eta^2\rangle = (\rho_a - \rho_c)^2\chi(1 - \chi) \tag{15}$$

The ρ, χ, and $\langle\eta^2\rangle$ values for the nylon 66 fiber are given in Tables IV–VI.

Mean Polarizability of Monomer Unit

For a bulk polymer of density ρ and monomer unit molecular weight M, the number of monomer units per unit volume v is $(N_A\rho)/M$, where N_A is 6.02×10^{23} and the M for nylon 66 is 226.

Because the refractive index of a polymer depends on the total polarizability of the molecules, this leads to the Lorentz–Lorenz equation by the following equations[28]:

$$\frac{n_\parallel^2 - 1}{n_\parallel^2 + 2} = \frac{v\alpha^\parallel}{3\Psi} \tag{16}$$

with analogous formula used for $n_a^\perp$, where $n_a^\parallel$ and $n_a^\perp$ are the mean refractive indices of the fiber for light vibrating parallel and perpendicular to the direction of the fiber axis, respectively; and Ψ is the permittivity of free space (8.85×10^{-12} Fm^{-1}).

$$\frac{\bar{n}^2 - 1}{\bar{n}^2 + 2} = \frac{v\bar{\alpha}}{3\Psi} \tag{17}$$

where $\bar{n}$ is the isotropic refractive index, $\bar{\alpha}$ is the mean polarizability of a monomer unit, and v is the number of carriers of the dipole moment.

De Vries[27] gave a theory on the basis of the internal field with the aid of classical electromagnetic theory, in which he generalized the Lo-

Table V

Draw Ratio	$n_{iso(1)}$	$n_{iso(2)}$	F_a	ρ	χ (%)	$\langle\eta^2\rangle \times 10^{-2}$	tan θ'
1.00	1.545	1.543	0.7641	1.1225	2.206	2.90	0.5177
1.08	1.544	1.542	0.8128	1.1225	2.153	2.84	0.4612
1.16	1.543	1.541	0.8423	1.1224	2.118	2.79	0.4144
1.32	1.543	1.541	0.9127	1.1223	2.032	2.68	0.3414
1.48	1.545	1.543	0.8864	1.1224	2.062	2.72	0.2875
1.56	1.543	1.541	0.9221	1.1223	2.015	2.66	0.2657
1.96	1.543	1.541	0.9475	1.1223	1.977	2.61	0.1886
2.12	1.544	1.543	1.0192	1.1222	1.884	2.49	0.1677
2.28	1.544	1.543	1.0471	1.1221	1.844	2.44	0.1503
2.44	1.544	1.542	1.0807	1.1220	1.795	2.37	0.1358

Table VI

Draw Ratio	$n_{iso(1)}$	$n_{iso(2)}$	F_a	ρ	χ (%)	$\langle\eta^2\rangle \times 10^{-2}$	tan θ'
1.000	1.547	1.545	0.4873	1.1224	2.112	2.78	0.5081
1.160	1.545	1.543	0.4859	1.1223	2.063	2.72	0.4067
1.320	1.544	1.542	0.4851	1.223	2.030	2.68	0.3350
1.480	1.543	1.541	0.4844	1.1222	1.917	2.53	0.2822
1.640	1.543	1.541	0.4841	1.1221	1.884	2.49	0.2419
1.880	1.542	1.541	0.4838	1.1221	1.851	2.45	0.1971
1.960	1.542	1.540	0.4833	1.1221	1.814	2.40	0.1852
2.040	1.543	1.542	0.4845	1.1221	1.816	2.40	0.1744
2.120	1.546	1.544	0.4871	1.1218	1.606	2.13	0.1646

rentz–Lorenz equation. Thus, for monochromatic light, the well-known Lorentz–Lorenz equation becomes the same as eq. (4). The right-hand member of eq. (4) is proportional to the ρ (g/m^3) of the medium and may also be written as

$$\frac{\bar{n}^2 - 1}{\bar{n}^2 + 2} = \bar{\varepsilon}\rho \tag{18}$$

where $\bar{\varepsilon}$ (m^3/kg) is the specific refractivity of the isotropic dielectric. Writing this equation for fibers in its parallel and transverse components, the generalized Lorentz–Lorenz equations are found:

$$\frac{n_\parallel^2 - 1}{n_\parallel^2 + 2} = \frac{v\alpha^\parallel}{3\Psi} = \varepsilon_\parallel\rho \tag{19}$$

An analogous formula is used for $n_a^\perp$.

The harmonic mean polarizability of the dielectric (α_v) is ascertained by the following equation:

$$\alpha_v = \frac{3\Psi}{v}\frac{n_v^2 - 1}{n_v^2 + 2} \tag{20}$$

Likewise, for the harmonic mean specific refractivity we have

$$\varepsilon_v = \rho^{-1}\frac{n_v^2 - 1}{n_v^2 + 2} \tag{21}$$

Birefringence of Homogeneously Uniaxially Stretched Polymer

From the above equation it can be seen that the birefringence in elastomers is proportional to the applied stress.[22] When the contributions of the chains to the network anisotropy are summed and the Lorentz–Lorenz relation is used to obtain the birefringence between the refractive index parallel to the extension direction $n^\parallel$ and the perpendicular $n^\perp$, the result is

$$n^\parallel - n^\perp = \frac{N'\gamma_s}{90\Psi}\frac{[\bar{n}^2 + 2]^2}{\bar{n}}[D^2 - D^{-1}] \tag{22}$$

where N' is the number of chains between crosslinks per unit volume at absolute temperature and γ_s is the segment anisotropy.

$$C_s = \frac{\gamma_s}{90\Psi kT}\frac{[\bar{n}^2 + 2]^2}{\bar{n}} \tag{23}$$

From eqs. (22) and (23) we can determine γ_s and then N'.

With the assumption that partially crystalline polymers consist of separate crystalline and amorphous phases, the change in the crystal direction on stretching was connected to the deformation of the amorphous matrix but the crystals did not change in size on stretching. The crystal c axis (the direction of the polymer chains in the crystal) and the stretching direction is given by[22]

$$\tan\theta' = D^{-3/2}\tan\theta \tag{24}$$

The angles θ and θ' are respectively before and after deformation on stretching. The values of tan θ' at different draw ratio values are summarized in Tables IV–VI.

The average orientation angle on the uniaxial stretching extension ratio D is

$$\langle \cos^2\theta_c \rangle = \frac{D^3}{D^3 - 1}\left|1 - \frac{\tan^{-1}(D^3 - 1)^{1/2}}{(D^3 - 1)^{1/2}}\right| \quad (25)$$

If there are Y crystals per unit volume and these have polarizabilities α_c along the c axis and $\alpha_b = \alpha_a$ perpendicular to it, then the crystal contribution to the birefringence of the medium is given by

$$[n^{\parallel} - n^{\perp}] = \frac{[\bar{n}^2 + -2]}{\bar{n}} \frac{Y}{18\Psi_o}[\alpha^{\parallel} - \alpha^{\perp}]\langle P_2(\cos^2\theta_c)\rangle \quad (26)$$

$$P_2(\cos^2\theta_c) = 1/2(3\cos^2\theta_c - 1) \quad (27)$$

Relation among Tension, Shear, Bulk Modulus, and Dipole Moment

A three-way equation may be written relating the four basic mechanical properties[29]:

$$E = 3B(1 - 2\mu) = 2(1 + \mu)G \quad (28)$$

where E is the tension, B is the bulk modulus, μ is the dipole moment, and G is the shear. Any two of these properties may be varied independently; conversely, acknowledgment of any two defines the other two. There is an especially important relationship when $\mu \cong 0.5$. The moduli of elasticity in E and G are related by the simple equation[30,31]

$$E \cong 3G \quad (29)$$

which defines the relationship between E and G to a good approximation for elastomers.

Rearranging the two left-hand portions in eq. (28) we have

$$1 - 2\mu = E/3B = \beta E/3 \quad (30)$$

where β is the compressibility.

Calculation of Density of Drawn Fibers

The actual draw ratio, which describes the actual dimensional changes, is related to density changes. For cylindrical fibers, the mass M can be expressed as

$$M = \rho V = \rho(\pi r^2 l) \quad (31)$$

where as V is the fiber volume. Assuming constant mass before (M_u) and after (M_d) drawing the actual D is given by the following equations:

$$\rho_u[\pi(r_u)^2 l_u] = \rho_d[\pi(r_d)^2 l_d] \quad (32)$$

$$D = \frac{l_d}{l_u} = \frac{(r_u)^2\rho_u}{(r_d)^2\rho_d} \quad (33)$$

$$\rho_d = \frac{(r_u)^2\rho_u}{(r_d)^2 D} \quad (34)$$

There are many properties commonly used to determine a degree of crystallinity, such as the density, heat of fusion, X-ray scattering, IR absorption, nuclear magnetic resonance line width, and so forth. Each of these properties gives somewhat different values for χ, but generally they will order samples with varying χ in the same sequence.

Thus, we used eq. (34) in our present work for the evaluation of the crystallinity of cold drawn nylon 66 fibers because it was the available technique at the time.

However, in this article we determine the crystallinity changes with the draw ratio with the above-described technique, and we do not claim that these results present the exact degree of crystallinity.

Calculation of Poisson's Ratio

The changes of the fiber radius and hence the cross-sectional area could be calculated with fair accuracy by the following expressions. To calculate these changes we can assume that the volume is constant by loading the sample. Hence, the change of the cross-sectional area of the fiber (ΔA) may be calculated from the relation

$$\Delta A = (A\Delta l)/(l + \Delta l) \quad (35)$$

where l is the initial length and Δl is the elongation that is produced. As a special case for fibers of very small radius contraction (Δr) by loading and on the base of the assumption of constant volume, the Δr may be calculated from the approximate formula

$$\Delta r = (r\Delta l)/2(l + \Delta l) \quad (36a)$$

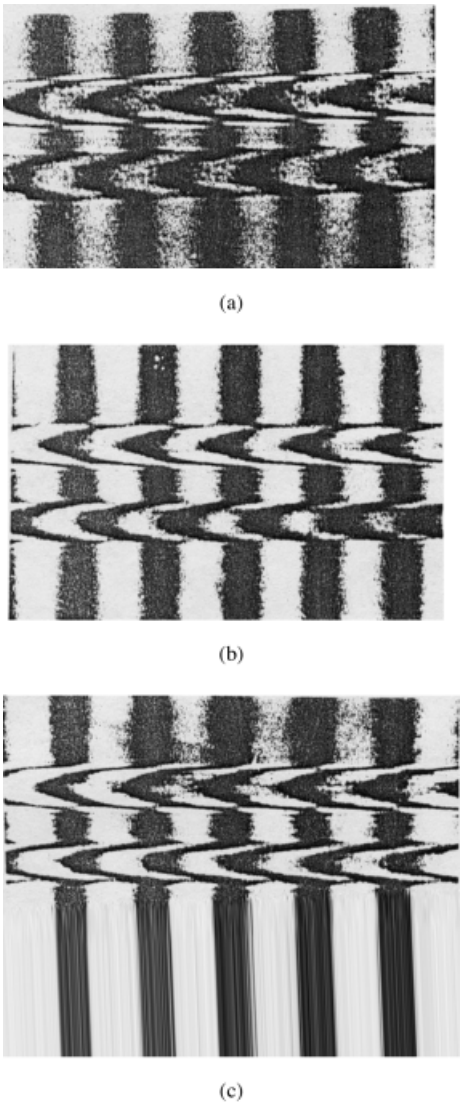

Figure 1 (a–c) Microinterferograms of two-beam interferometry from the totally duplicated image of nylon 66 fiber at different draw ratios (λ = 546 nm).

where r is the radius of the unloaded fiber. Introducing the value of Δr given in eq. (35) into the well-known definition of Poisson's ratio (μ) for fibers of very small Δr we obtain

$$\mu = -\frac{\Delta r/r}{\Delta l/l} = \frac{l}{2(l + \Delta l)} = \frac{1}{2D} \tag{36b}$$

where $D = (l + \Delta l)/l$ is the draw ratio.

Calculation of Isotropic Refractive Index

The isotropic refractive index (n_{iso}) is given by the equation

$$n_{\text{iso}} = \frac{[n_a^{\parallel} + 2n_a^{\perp}]}{3} \tag{37}$$

from which the specific V is given by the relation

$$(n_{\text{iso}} - 1)V = \text{const} \tag{38}$$

In addition, the Lorentz–Lorenz equation is used to correlate the polarizabilities and refractive index as follows[30]:

$$\frac{n_{\text{iso}_{(2)}}^2 - 1}{n_{\text{iso}_{(2)}}^2 + 2} = \frac{1}{3}\frac{\rho_i}{\rho}\left[\frac{n^2 - 1}{n^2 + 2} + 2\,\frac{n_{\perp}^2 - 1}{n_{\perp}^2 + 2}\right] \tag{39}$$

where ρ and ρ_i are the densities measurement and the isotropic polymer, respectively; and $\rho_i = \rho_a = 1.12$ g/mL. The value of $n_{\text{iso}_{(1)}}$ and $n_{\text{iso}_{(2)}}$ for nylon 66 fiber are given in Table IV–VI.

Calculation of Molar Refractivity

The polarizability of a molecule is related to its refractive index[31] by the Lorentz–Lorenz relation:

$$\frac{\bar{n}^2 - 1}{\bar{n}^2 + 2}\frac{M}{\rho} = \frac{4}{3}\pi N_A \bar{\alpha} = R \tag{40}$$

where R is the molecular or molar refractivity and the value of M used is that of the repeat unit of the molecule.

Calculation of Cohesive Energy Density and Square Solubility Parameters

The value of the B was calculated in terms of the cohesive energy density (CED), which represents the energy theoretically required to move a detached segment into the vapor phase. This in turn is related to the square of the solubility parameter.[32]

$$B = 8.04\ (\text{CED}) \tag{41a}$$

$$B = 8.04\delta^2 \tag{41b}$$

The factor 8.04 arises from Lennard–Jones considerations.

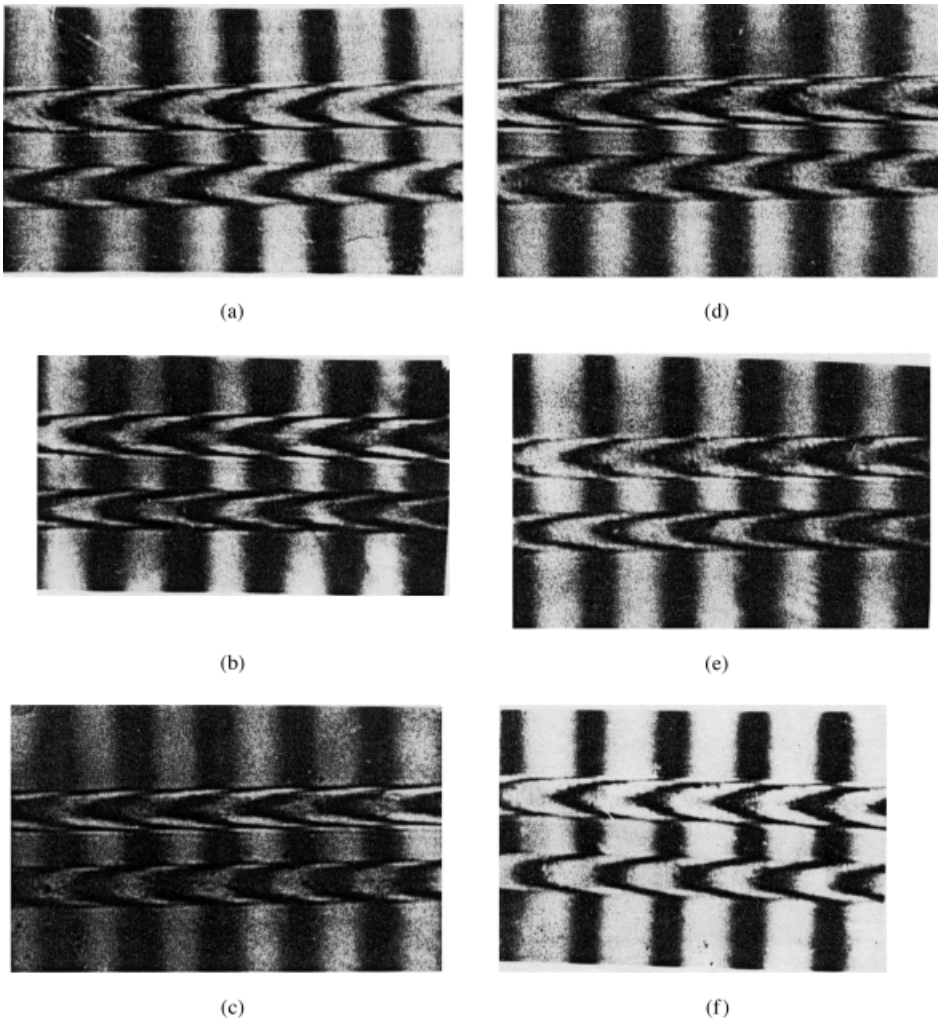

Figure 2 (a–f) Microinterferograms of two-beam interferometry from the totally duplicated image of nylon 66 fiber at different draw ratios (λ = 546 nm).

RESULTS

Sample Preparation

Annealing Process

The nylon 66 fibers were wound in a cocoon form on a glass rods with free ends, and then they were annealed in an electric oven. The temperature was adjusted to 90 and 110 ± 1°C with constant annealing times of 4 h and then left to cool in air at 28 ± 1°C.

Application of Two-Beam Interferometry

The totally duplicated image of the fiber obtained with a Pluta polarizing interference microscope was used to calculate the mean refractive indices $n_a^{\parallel}$ and $n_a^{\perp}$ of nylon 66 fibers.

Figures 1(a–c) and 2(a–c) are microinterferograms of the totally duplicated images for unannealed and annealed nylon 66 fibers, respectively, using the Pluta microscope with different draw ratios before and after the annealing temperatures. Figures 1 and 2 also show that the fringe shifts change as the annealing temperature and drawing increase. Using these interferograms, the mean refractive index in the parallel and perpendicular directions at different annealing temperatures and constant annealing time were calculated.

Tables I–III give the calculated values for the N_c, N', B, E, σ, C_s, and Δa at different draw ratios for annealing nylon 66 fibers. Tables IV–VI give the calculated values for the $\bar{n}$, ρ, and χ at different draw ratios for unannealed and annealed nylon 66 fibers.

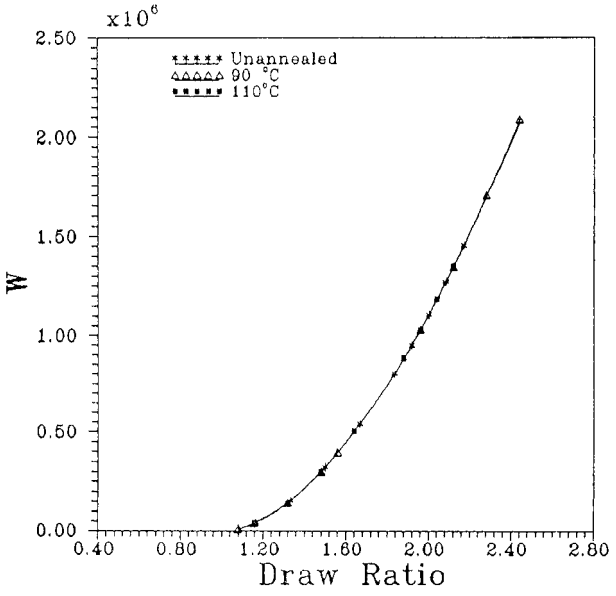

Figure 3 The relation between the work per unit volume (W) and the draw ratios of nylon 66 fiber with annealing temperatures of 90 and 110°C.

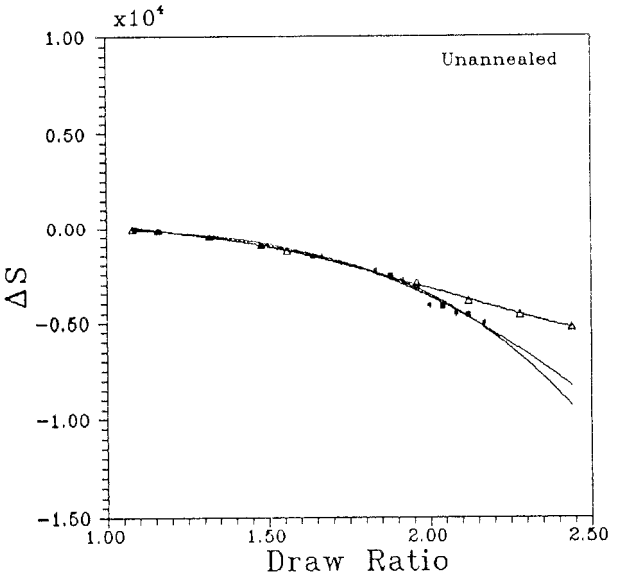

Figure 5 The relation between the birefringence (ΔS) and the draw ratios of nylon 66 fiber with annealing temperatures of 90 and 110°C.

Figure 3 shows the relationship between the W and the draw ratio for unannealed and annealed nylon 66 fibers. The relationship between the W' and the draw ratios for unannealed and annealed nylon 66 fibers are shown in Figure 4. Figure 5 shows the relationship between the ΔS and the draw ratios for unannealed and annealed nylon 66 fibers, and Figure 6 shows the relationship between the Δn_a and the ΔS under different annealing conditions and different draw ratios. The relationship between the μ and the draw ratios at different annealing conditions for nylon 66 fibers

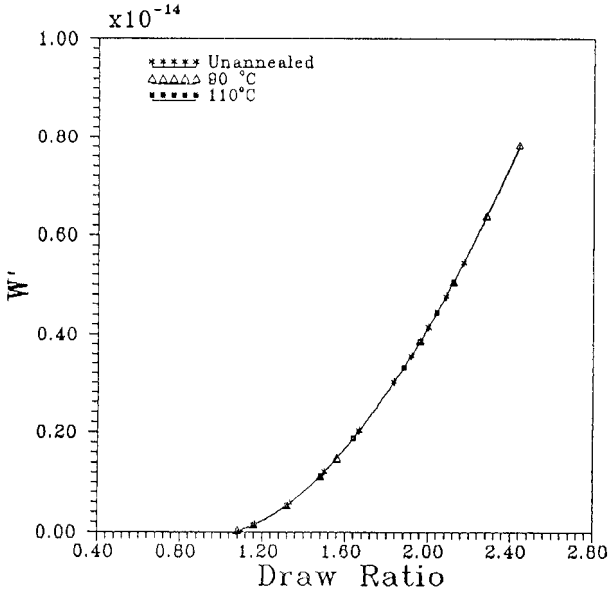

Figure 4 The relation between the average work per chain (W') and the draw ratios of nylon 66 fiber with annealing temperatures of 90 and 110°C.

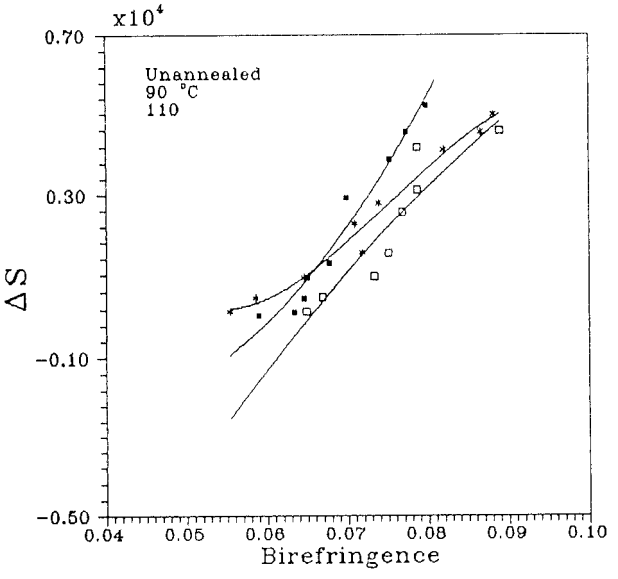

Figure 6 The relation between the birefringence (Δn) and the entropy (ΔS) of nylon 66 fiber at different draw ratios with annealing temperatures of 90 and 110°C.

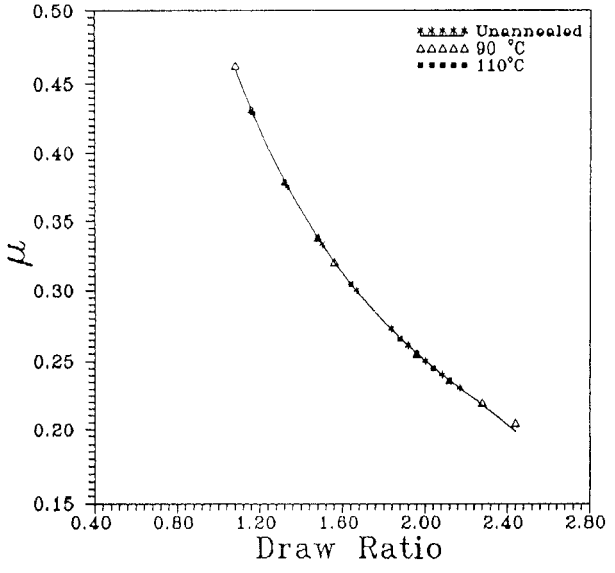

Figure 7 The relation between Poisson's ratio (μ) and the draw ratios of nylon 66 fiber with annealing temperatures of 90 and 110°C.

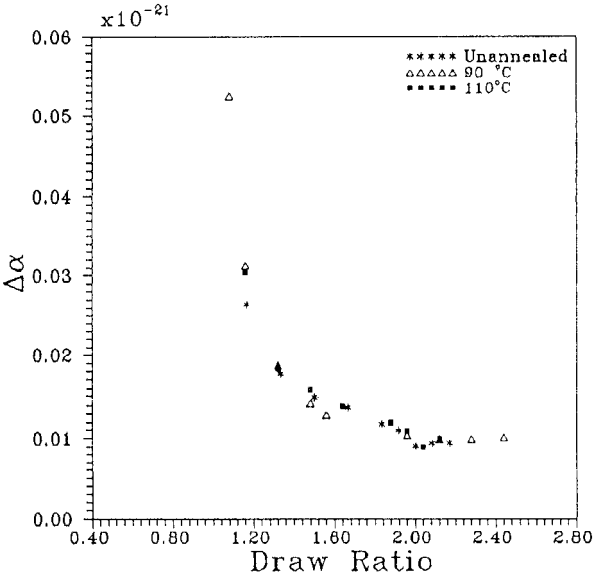

Figure 9 The relationship between the optical configuration parameter (Δa) and the draw ratios of nylon 66 fiber with annealing temperatures of 90 and 110°C.

is presented in Figure 7. Figure 8 describes the relationship between the C_s and the draw ratios with different annealing conditions for nylon 66 fibers, and Figure 9 shows the relationship between the Δa and the draw ratios at different annealing conditions for the fibers.

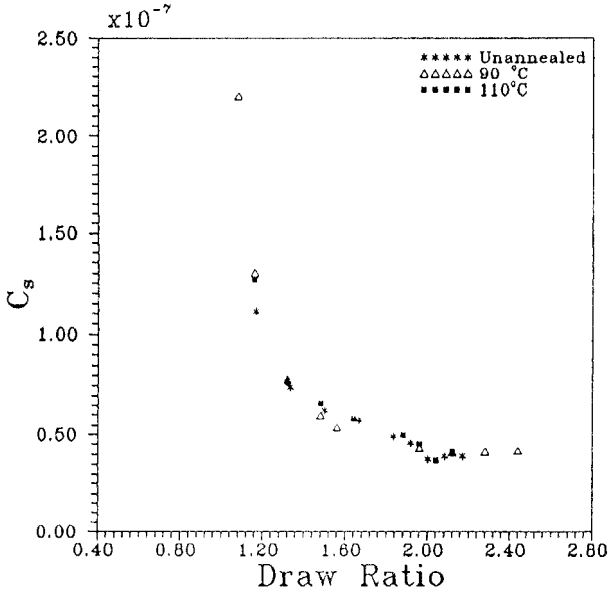

Figure 8 The relation between the optical stress coefficient (C_s) and the draw ratios of nylon 66 fiber with annealing temperatures of 90 and 110°C.

DISCUSSION

Part of the modern trend in fiber research is to alter the fiber properties. One of the methods for property modification involves the effects of an annealing process and then cold drawing under different conditions. Several studies have been reported on the effects of annealing and mechanical processes on the structure of synthetic and natural fibers. Birefringence orientation, density, crystallinity, and elasticity are some of the properties that affect textile quality for the main end use. Thus, the determination of the density constitutes a fair method for determining the percentage of crystallinity. Density measurements can also be used to follow the continuous changes occurring during the physical changes of the samples under investigation. The values of the evaluated crystallinity that are attained are very dependent on the nature of the polymer and its thermal and mechanical treatments.[33–36]

Under annealing and cold drawing conditions and following the obtained optical and mechanical parameters results, a polymeric material was obtained with modified physical properties that were due to the changes in the ΔS, CED, δ^2, μ, E, and optical parameters. Also, to explain the different variations obtained because of thermomechanical effects, there are several structural processes that interfered that should be taken into

consideration, which are discussed elsewhere.[37–39] Although the degree of orientation always increases in the course of drawing, crystallinity can change in both directions. Three types of behavior can be distinguished: Deformation does not affect the phase structure of an undrawn amorphous sample after drawing, and a crystalline sample does not change its degree of crystallinity; deformation is accompanied by partial destruction of the original structure and reduction of the crystallinity; and deformation is accompanied by additional crystallization and an increase of the crystallinity.

Thus, the present results show a reduction of the crystallinity, which may be due to drastic distortion of the original structure of the amorphous material due to cold drawing.[40]

CONCLUSIONS

It is clear from the above measurements and calculations of the various optical density and mechanical parameters and their changes with annealing and cold drawing processes that the following conclusions can be drawn:

1. Clearly there are isothermal kinetic changes due to the drawing process that are confirmed by the ΔS changes, which are accompanied by changes of the Δn (birefringence). Also, the retractive forces of the network are produced by the decrease in entropies of freely jointed chains when stretched.
2. A changes of the ΔS, CED, and δ^2 throw light on the energies, which play a role in clarifying the phase boundary between the amorphous and crystalline regions.
3. Application of the Moony–Rivlin equation shows a linear relationship. The constants C_1 and C_2 are determined and found to be, respectively.
4. It is clear that there are changes in the calculated values of the isotropic refractive indices due to the application of different formulas; every equation has its own merit because of its available technique.
5. Annealing and cold drawing cause the crystallinity to decrease as increases oriente the polymer fiber (Tables IV–VI, i.e., the orientation is the result of deformation).
6. Changes of the crystallinity are accompanied by changes of mass redistribution within the fiber chains. This also indicates the changes of the chain (segmental) orientation, which is the result of deformation.
7. Calculating the degree of crystallinity using eq. (14) leads to evaluating and explaining many structural parameters (i.e., $\alpha_{\|}$, $\alpha_{\perp}$, α_{v}, $\varepsilon_{\|}$, $\varepsilon_{\perp}$, ε_{v}, n_{iso}, etc.).

From the above results and considerations we concluded that the practical importance of these values provides acceptable evaluations for the thermomechanical optical parameters changes for nylon 66 fibers.

REFERENCES

1. Barakat, N. Text Res J 1971, 41, 391.
2. Barakat, N.; Hamza, A. A. Interferometry of Fibrous Materials; Hilger: Bristol, U.K., 1990.
3. Samules, J. R. Structural Polymer Properties; Wiley: New York, 1974; Vol. 20, p 50.
4. Fouda, I. M.; El-Tonsy, M. M.; Hosny, H. M. Polym Degrad Stabil 1994, 46, 287.
5. Fouda, I. M.; El-Tonsy, M. M. J Mater Sci 1990, 25, 121.
6. Hamza, A. A.; Fouda, I. M.; Kabeel, M. A.; Shabana, H. M. Polym Test 1996, 15, 35.
7. Fouda, I. M.; Seisa, E. A. J Polym Polym Compos 1996, 4, 247.
8. Fouda, I. M.; El-Nicklawy, M. M.; Naser, E. M.; El-Agamy, R. M. J Appl Polym Sci 1996, 60, 1247.
9. Vallat, M. F.; Plazek, D. J.; Bhushan, B. J Polym Sci Part B Polym Phys 1988, 26, 555.
10. Hamza, A. A.; Sokkar, T. Z. N.; Kabeel, M. A. J Phys D Appl Phys 1985, 18, 2321.
11. Polukhin, P.; Gorelik, S.; Vortontsov, V. Physical Principals of Plastic Deformation; Mir: Moscow, 1983; p 275.
12. Zachariodes, A. Z.; Porter, S. R. The Strength and Stiffness of Polymers; Marcel Dekker: New York, 1983; p 121.
13. Bassett, D. C. Principles of Polymer Morphology; Cambridge University Press, Cambridge, U.K., 1981; p 124.
14. Hamza, A. A.; El-Farahaty, K. A.; Helaly, S. A. Opt Applic 1988, XVIII, 133.
15. Hamza, A. A.; Fouda, I. M.; El-Tonsy, M. M.; El-Sharkawy, F. M. J Appl Polym Sci 1995, 56, 1585.
16. Hamza, A. A.; Fouda, I. M.; Kabeel, M. A.; Seisa, E. A.; El-Sharkawy, F. M. J Appl Polym Sci 1998, 67, 1957.
17. Hamza, A. A.; Fouda, I. M.; Kabeel, M. A.; Seisa, E. A.; El-Sharkawy, F. M. Polym Test 1997, 16, 303.

18. Fouda, I. M.; Kabeel, M. A.; El-Sharkawy, F. M. Polym Polym Compos 1997, 5, 431.
19. Stein, R. S. J Polym Sci 1959, 24, 709.
20. Hermans, P. H. Contributions to The Physics of Cellulose Fibers; North Holland: Amsterdam, 1946.
21. (a) Monney, M. J Appl Phys 1940, 11, 582; (b) Monney, M. J Appl Phys 1948, 19, 379; (c) Sperling, L. H. Introduction to Physical Polymer Science, 2nd ed.; Wiley: New York, 1992.
22. Jenkins, A. D. Materials Science Handbook, Polymer Science; Amsterdam: North-Holland, 1972; Vol. 1, p 505.
23. Williams, D. J. Polymer Science, and Engineering; Prentice–Hall: London, 1971; p 190.
24. Riande, E.; Guzman, J. J Polym Sci Phys Ed 1984, 22, 917.
25. Le Borurvellee, G.; Beautemps, J. J Appl Polym Sci 1990, 39, 329.
26. Brandrup, J.; Immergut, E. H. Polymer Handbook, 2nd ed.; Wiley: New York, 1975; p 779.
27. Fischer, E. W.; Fakirov, S. J Mater Sci 1975, 11, 955.
28. de Vries, H. Z Colloid Polym Sci 1979, 257, 226.
29. Sperling, L. H. Introduction to Physical Polymer Science, 2nd ed.; Wiley: New York, 1992; p 161.
30. Cunningham, A.; Ward, I. M.; Willis, H. A.; Zichy, V. Polymer 1974, 15, 749.
31. Hemsley, D. A. Applied Polymer Light Microscopy, Elsevier: London, 1964; p 88.
32. Vinogradov, G. V.; Ozyara, E. A.; Malkin, A. Y.; Grechanovskü, V. A. J Polym Sci 1971, A-2, 1153.
33. Fouda, I. M. Polym Test 1999, 18, 363.
34. Fouda, I. M.; Shabana, H. M. Polym Int 1999, 48, 602.
35. Fouda, I. M.; Shabana, H. M. Polym Polym Compos 1999, 7, 333.
36. Fouda, I. M.; El-Sharkawy, F. M. Polym Polym Compos 1999, 7, 355.
37. Fouda, I. M.; Shabana, H. J Appl Polym Sci 1999, 72, 1185.
38. Fouda, I. M.; Shabana, H. M. Polym Int 1999, 48, 198.
39. Fouda, I. M.; Shabana, H. M. Polym Polym Compos 2000, 8, 497.
40. Walezak, Z. K. Formation of Synthetic Fibers; Gordon & Breech: New York, 1977; p 418.